

Effect of Long Branching and Strain-Induced Crystallization of *cis*-1,4-Polybutadiene Observed in Nonlinear Viscoelastic Behavior

N. NAKAJIMA* and Y. YAMAGUCHI†

Institute of Polymer Engineering, The University of Akron, Akron, Ohio 44325-0301

SYNOPSIS

The effect of long branching on the deformational behavior has been examined for four commercial high *cis*-polybutadienes with particular interest as to its implication on their processability. The techniques used were oscillatory shear measurements at small deformation and tensile stress-strain measurements at large deformation. In the shear measurements (linear behavior), the temperature dependence of the shift factor in the time-temperature superposition is related to the degree of branching obtained from dilute solution viscosity. In the tensile measurements (nonlinear behavior), the rubbers showed either strain-hardening or strain-softening. The difference was not related to the degree of branching determined by dilute solution viscosities. This means that the dilute solution viscosity is not an adequate means to explain the processability difference of the rubbers. The branch length, although the absolute value is unknown, is characterized as short or long on the basis of the strain-softening or strain-hardening behavior. Both small shear and large elongational measurements are necessary for characterization of branching pattern and processability. Rubbers with relatively short branches (strain-softening type) or with the smallest amount of long-branching (non-strain-hardening type) were found to strain-crystallize most easily. The absence of strong resistance to stretching is the apparent reason for the ease of crystallization. © 1996 John Wiley & Sons, Inc.

INTRODUCTION

cis-1,4-polybutadiene is one of the most widely used elastomers in industry. Many grades of *cis*-polybutadiene have been developed in order to improve processability and performance. Structural variables include molecular weight, molecular weight distribution, long-chain-branch content, and branching pattern.

The influence of molecular structure on rheological properties has been investigated systematically with some model polymers.¹⁻⁴ Typical examples of model polymers are "monodispersed" linear or star-branched structures. The model polymers of the polybutadienes had a microstructure consisting of mixtures of *cis*-, *trans*-, and vinyl-isomers. Experimental methods were steady shear and linear viscoelastic measurements. However, these methods are not satisfactory in two respects for understanding the processing of elastomers: first, the commercial rubbers are very different from the model polymers; *cis*-polybutadienes have a broad molecular weight distribution and sometimes long branches, and also, the branch pattern is more complex than a star; second, the processing conditions are not in steady shear, nor is the rubber behavior linearly viscoelastic.

Processing of elastomers involves small (linear) and large (non-linear) deformation in both shear

This article is based on a paper presented at 147th meeting of The Rubber Division, American Chemical Society, Philadelphia, PA, May 2-5, 1995.

* To whom correspondence should be addressed: Institute of Polymer Engineering, The University of Akron, College of Polymer Science & Polymer Engineering, Akron, OH 44325-0301.

† Present address: Yokohama Rubber Co., 1-2 Oiwake, Hiratsuka 254, Japan.

Journal of Applied Polymer Science, Vol. 61, 1525-1539 (1996)

© 1996 John Wiley & Sons, Inc.

CCC 0021-8995/96/091525-15

Table I Samples^a

Sample	Catalyst	<i>cis</i> -1.4 (%)	1.2-Vinyl (%)	$M_w^c \cdot 10^{-4}$	$M_n^c \cdot 10^{-4}$	M_w/M_n^c	MV ^d	T_g (°C)	Degree of Branching ^e (%)
BUNA CB11 ^b	Ti	93	4	51	12	4.3	47	-105	10
BUNA CB22 ^b	Nd	98	1	53	20.5	2.6	63	-109	5
BUNA CB23 ^b	Nd	98	1	51.5	15	3.4	51	-109	5
BUNA CB24 ^b	Nd	98	1	66.5	12	5.5	44	-109	3

^a All data supplied by the manufacturer.

^b Registered trade mark of Bayer AG.

^c The data by GPC; molecular weights are not absolute, but relative values based on the hydrodynamically equivalent volume of polystyrene standards.

^d Mooney viscosity.

^e Calibrated with star-branched polymers.

and elongation. Moreover, these deformations include non-steady, transient states. Rubbers often show different behavior at large deformation not expected from small deformation; for example, strain-hardening or strain-induced crystallization.

In the previous work⁵⁻⁸ with NBR, SBR, EP(D)M, poly(ethyl acrylate) and others, oscillatory shear measurements were used for evaluating the linear behavior, and tensile stress-strain measurements were used for evaluating the nonlinear behavior. These rubbers, with the exception of EP(D)M, were produced by emulsion-polymerization with a free-radical reaction and had long branches forming gels. Long branches and gels were

found to be the major structural variables controlling the material behavior. On the other hand, *cis*-polybutadiene is produced by solution polymerization and has a smaller amount of long branches. Its branching pattern may also be different from that in the emulsion rubbers. In this work, we apply the procedure used in the previous works⁵⁻⁸ to high *cis*-polybutadiene to find the effect of branching on the deformational behavior.

The currently available analytical techniques are not sensitive enough to give absolute values of the number and length of branches. The conventional method of assigning "a degree of branching" through the dilute solution method does not provide the

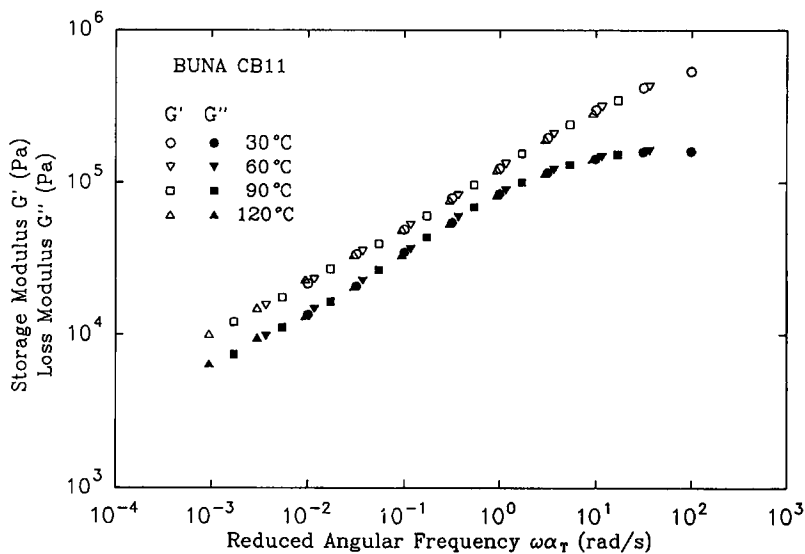


Figure 1 Master curves of storage and loss modulus of CB11. (Reference temperature 30°C).

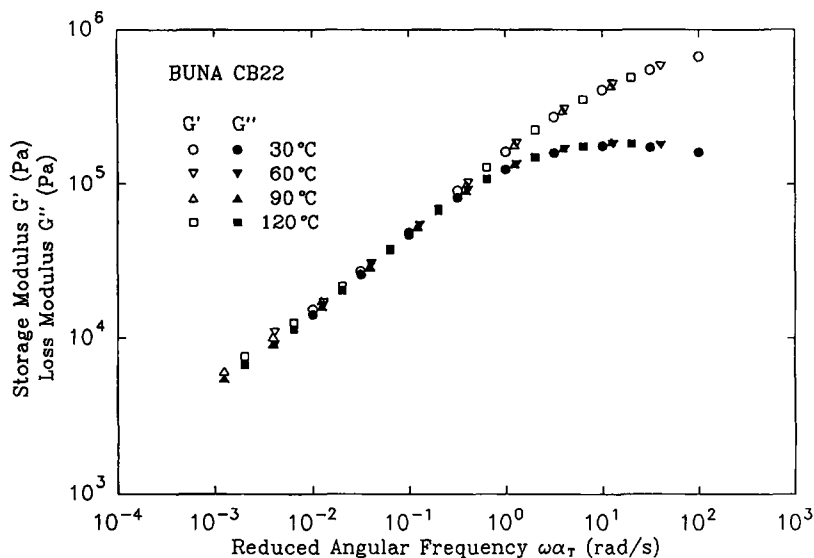


Figure 2 Master curves of storage and loss modulus of CB22. (Reference temperature 30°C).

above information. Based on our previous experience in viscoelastic characterization of commercial rubbers,⁵⁻⁸ there is a possibility of obtaining information on the number and length of long branches, even though the information is a relative one, from the nonlinear viscoelastic behavior. The latter, of course, describes the processability of a given rubber. This work applies nonlinear viscoelastic analysis to high *cis*-polybutadiene with particular attention to the nature of long branching and its relation to strain-

induced crystallization. This is a subject of large commercial importance and it has not been critically examined before.

Mechanism of Branch Formation

In the emulsion polymerization of dienes with a free-radical initiator there is an inherent mechanism of chain transfer which results in the formation of long branches. The probability of chain transfer is higher

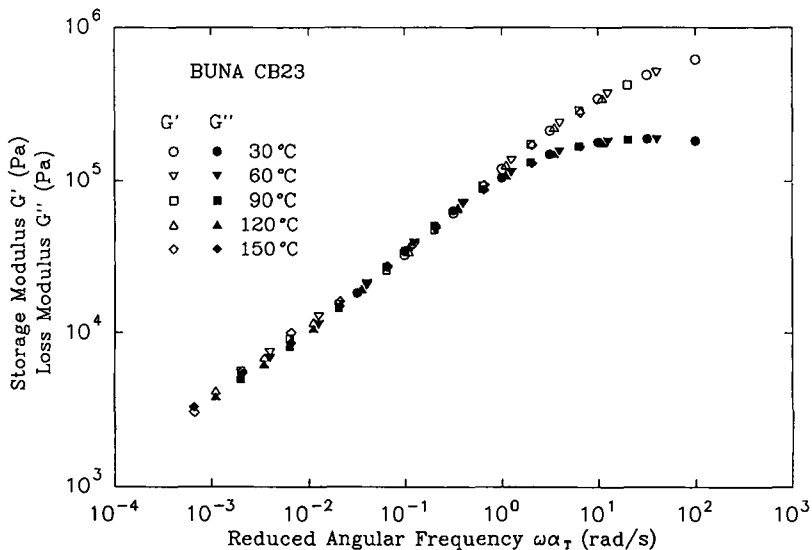


Figure 3 Master curves of storage and loss modulus of CB23. (Reference temperature 30°C).

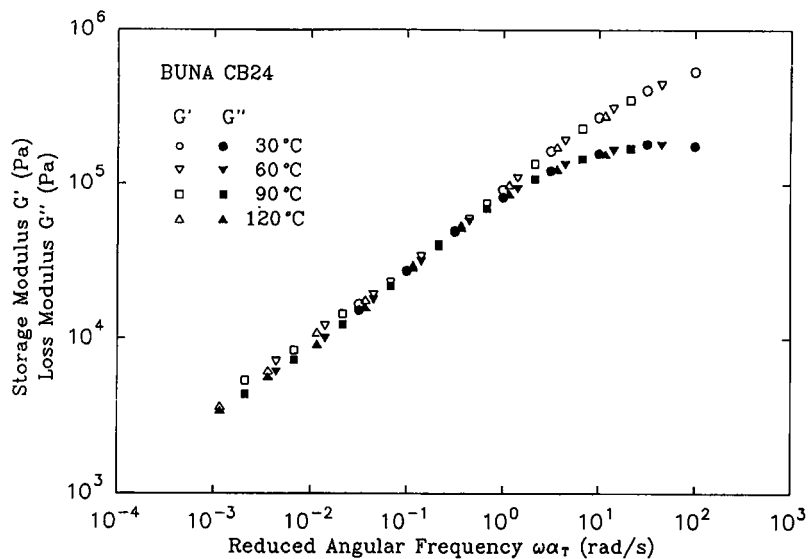


Figure 4 Master curves of storage and loss modulus of CB24. (Reference temperature 30°C).

for larger molecules, so that branched molecules become more branched. This results in the formation of a macrogel, which is an extensively branched molecule.^{9,10}

In solution polymerization employing non-free-radical initiators, such as the synthesis of high *cis*-1,4 polybutadiene, there is no chain transfer mechanism. The polymer chain grows through a sequential addition of the monomer inserted into the catalyst site. Thus, branch formation is a result of the insertion of a macromer. Once a macromer is in-

serted, the probability of another macromer insertion decreases because of the steric effect. Therefore, branch formation is self-restrictive and normally a gel does not form. Also, the shorter macromer is favored in the insertion so that the long branch may be shorter than that in emulsion polymerization. Of course, the degree and length of branching depend upon the availability of the macromer and the nature of the catalyst site. For example, cobalt-based *cis*-polybutadienes show significant branching with increased conversion¹¹ and the presence of chain in-

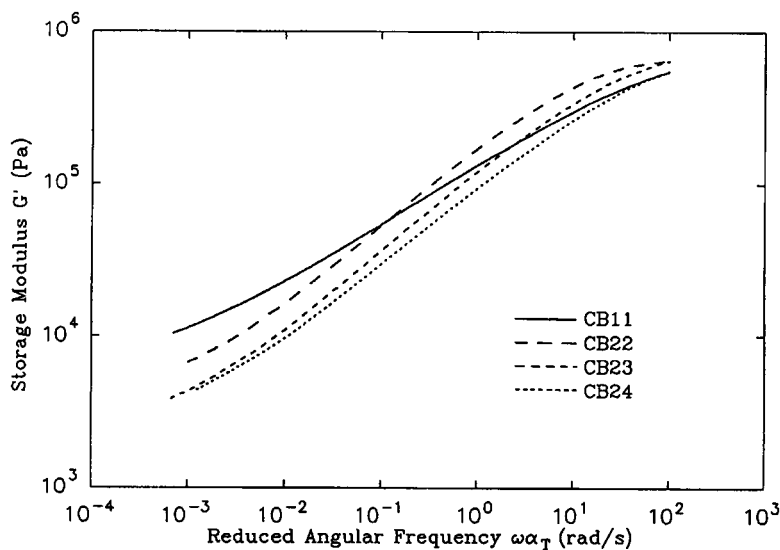


Figure 5 Comparison of master curves of storage modulus. (Reference temperature 30°C).

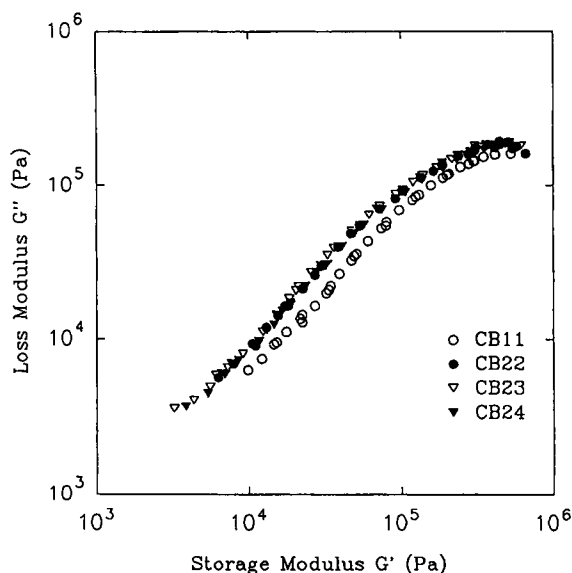


Figure 6 Comparison of $\log G''$ vs. $\log G'$ curves.

sersion to aluminum alkyl during polymerization was suggested for the neodymium catalyst system.¹² It has also been shown that degree of branching can be controlled by a use of a highly reactive catalyst and cocatalyst.¹³

Effect of Long Branching on Rheological Behavior

Kraus and Gruver² investigated the effect of branching on rheological behavior. Samples were polybutadienes having narrow molecular weight distribution of linear and star-branched structure. For low molecular weights the Newtonian viscosity, η_0 , of trichain or tetrachain star molecules was lower than that of linear polymer having the same molecular weight. For molecular weights higher than a critical value, the η_0 of the branched molecule was higher than the corresponding value for a linear polymer. This is called viscosity enhancement.

They explained these behaviors based on the relation of branch length to entanglement-spacing molecular weight, M_e . When the branches are not much longer than M_e , slippage of the entanglement does not offer a significant resistance to flow. When the branches are much longer than M_e (the critical branch length is $3 M_e$ for trichain and $4 M_e$ for tetrachain polymer²), the resistance to flow involves slippage of the entanglements of the branch as well as the main chain.

For molecular weight high enough to observe viscosity enhancement of the branched molecules, the viscosity enhancement diminishes with increasing

shear rate and eventually the viscosity of the branched molecule becomes lower than that of the linear equivalent. This is called viscosity reduction. This is interpreted to be the result of the slippage of the entanglements not recovering at the higher shear rates.¹⁴ Therefore, the branching "lubricates" the flow, resulting in the viscosity reduction.

Graessley¹⁵ explained the enhancement of η_0 of branched polymers with deGennes' reptation model.¹⁶ The reptating motion of the chain is considerably hindered by the presence of long branches which are "pinned" by a significant number of entanglements.

With commercial rubbers, η_0 is usually not observable because of their very high molecular weight, long branches, and gel. With rubbers having long branches and gel, the viscosity enhancement is observed at low shear rates. However, at high shear rates these rubbers tend to show the viscosity reduction.

The rubbers containing long branching and macrogel tend to exhibit strain-hardening upon stretching. When the branches are long enough, preventing the slipping of the entanglements, the constrained entanglements work as the resistance to deformation and induce the strain-hardening. When the branches are not long enough, the branches slip out from the entanglements easily upon stretching. Such a branch aligning with the main chain and the resulting lubrication facilitates stretching, i.e., the strain-softening.

Viscoelastic Characterization Methods

The oscillatory shear data are presented as the storage modulus, G' , and the loss modulus, G'' , as a function of frequency. From our previous experience we know that a degree of branching may be assessed from the relative position of the curves plotted as $\log G''$ vs. $\log G'$.¹⁷

The tensile stress-strain data may be presented as the modulus, E , as a function of strain, ϵ , and time, t ¹⁸:

$$E(\epsilon, t) = \sigma/\epsilon \quad (1)$$

where σ is the true stress based on the cross-sectional area of deformed specimen and ϵ is related to the extension ratio, α , as

$$\epsilon = \alpha - 1 \quad (2)$$

Table II Shift Factor α_T and β_T

	Sample	Temperature (°C)				
		30	60	90	120	150
α_T	CB11	1	0.368	0.171	0.094	0.052*
	CB22	1	0.409	0.202	0.124	0.071*
	CB23	1	0.400	0.202	0.111	0.066
	CB24	1	0.449	0.215	0.117	0.067*
β_T	CB11	1	0.934	0.834	0.794	—
	CB22	1	0.910	0.803	0.753	—
	CB23	1	0.893	0.844	0.734	0.660
	CB24	1	0.938	0.828	0.726	—
	$\rho_0 T_0 / \rho T$	1	0.910	0.835	0.771	0.716

* Slight degradation was noticed.

When the experiment is performed at a constant deformation rate, $\dot{\epsilon}$, the time and strain are related as

$$t = \epsilon / \dot{\epsilon} \quad (3)$$

With some rubbers a particular form of the strain-time correspondence principle is applicable and the modulus, E , is a function of reduced time, αt ,

$$\sigma / \epsilon = E(\alpha t) \quad (4)$$

where the strain-shift factor, α , is the extension ratio. Henceforth, eq. (4) is referred to as the strain-

time correspondence. When eq. (4) is applicable, the tensile stress-strain results obtained at different deformation rates can be superposed to form a master curve.

The modulus may be converted into a form of viscosity, η_T with $(1/\alpha t)$ being the reduced deformation rate,

$$3\eta_T = E(\alpha t)\alpha t \quad (5)$$

The factor 3 relates shear and elongation behavior for Poisson's ratio of 0.5. When eq. (4) results in the linearization of nonlinear data, η_T may be compared

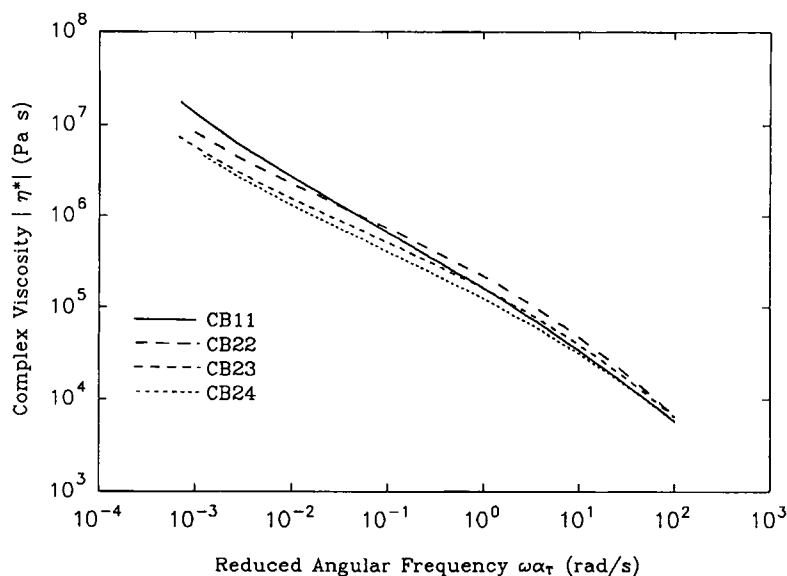


Figure 7 Comparison of master curves of complex viscosity. (Reference temperature 30°C).

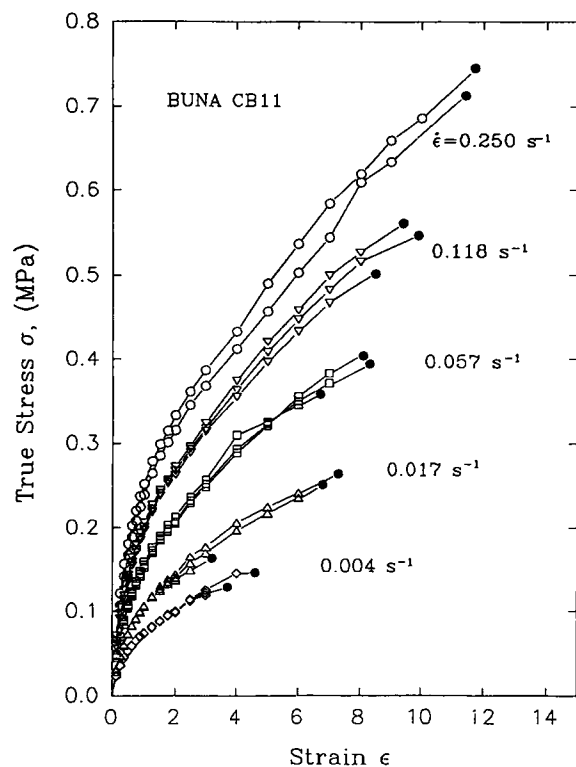


Figure 8 Tensile stress-strain curves of CB11.

to the absolute value of the complex viscosity, $|\eta^*|$, as

$$\eta_T = |\eta^*| \quad (6)$$

the viscosities being taken at equal value of the frequency, ω , rad/s and the rate, $1/\alpha t$.

Gel-free elastomers and elastomers containing microgel (a crosslinked particle) obey the above reduction scheme. However, elastomers containing macrogel (extensively branched molecule) do not obey, exhibiting strain-hardening. Subsequently, modulus shift is applied to obtain a master curve. Then, the modulus shift factor, $\Gamma(\alpha)$, is a measure of the strain-hardening¹⁹

$$3\eta_T = E(\alpha t)\alpha t/\Gamma(\alpha) \quad (7)$$

If the polymer contains polar moieties as a major component, then even with gel-free elastomers, a relation, $|\eta^*| < \eta_T$, was found.⁸ A polar association created upon stretching was postulated as a cause.

EXPERIMENTAL

Samples

The samples were four commercial polybutadienes produced by Bayer AG (Table I). The sheets of gum rubbers were prepared by pressing at 140°C for 10 min. After removing from the press, the sheets were cut in quarters, piled in four layers, and pressed again under the same conditions to completely remove bubbles. After the second pressing the sheets were placed between two steel plates at room temperature with heavy weights placed on top. The sheets were allowed to rest at least 2 days under the heavy weights in order to prevent wrinkling when removed.

Oscillatory shear specimens were cut from the sheets as discs 25 mm in diameter and tensile specimens were cut within ASTM D412 dumbbell die C.

The gel contents of the sheets were measured by dissolving about 0.4 g of rubber in 100 ml of *n*-heptane for 48 h. The solution was filtered through Whatman No. 4 filter paper. The filter paper was weighed before and after filtration to estimate the amount of gel removed from the solution. The filtered solution was evaporated in an oven at 110°C and the amount of dissolved polymer was measured.

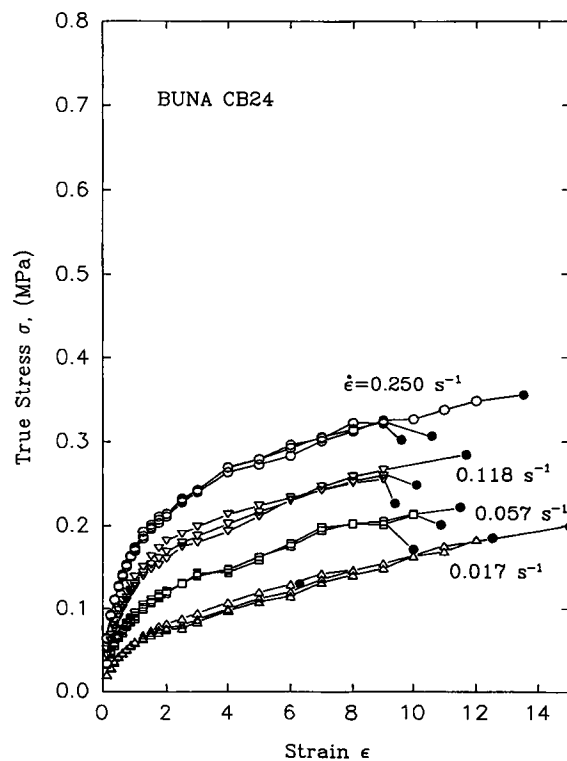


Figure 9 Tensile stress-strain curves of CB24.

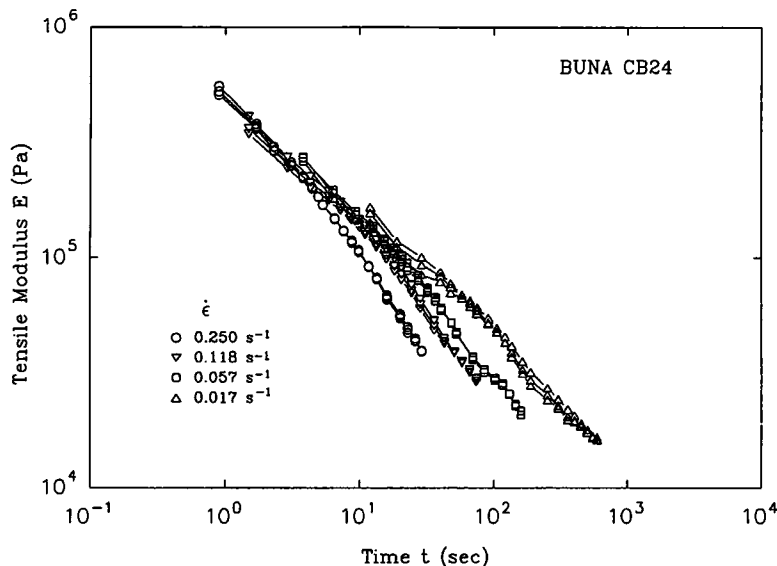


Figure 10 Tensile modulus as a function of time for CB24.

Instruments

The oscillatory shear measurements were performed with a Rheometrics Mechanical Spectrometer RMS800 with parallel plates. The angular frequency range was from 10^{-2} to 10^2 rad/s. The samples were tested at 30, 60, 90, 120, and 150°C . In addition to the calibration specified by the instrument manufacturer, a standard silicon rubber (SE30; General Electric Company) was used every time to double-check the calibration. The frequency sweep was made from the lowest to the highest and then reversed to the lowest frequency. The data at the lowest frequency should reproduce if there is no degradation during the measurements.

Tensile tests were performed with a Monsanto Tensometer 500. The strip chart recorder recorded force against time. The force was measured with a 0.45 kg load cell. The extent of deformation was measured by recording with a video camera. An extensometer was not used because the samples were not strong enough to hold it. The samples were held with plastic grips having relatively loose springs in order to prevent breaking at the grips. The tests were performed at room temperature with strain rates of 0.004, 0.017, 0.057, 0.118, and 0.250 s^{-1} .

RESULTS AND DISCUSSION

Oscillatory Shear Measurements

Time-temperature superposition was performed in the following sequence: first, $\tan \delta$ data were plotted

against $\log \omega$. The superposition involves the $\log \omega$ axis only, because any modulus-shift in G' and G'' cancels out. From this procedure the time-shift factor, α_T , was evaluated. Next, $\log |G^*|$ data were plotted against $\log \omega \alpha_T$. From these plots the modulus-shift factor, β_T , was evaluated. The results of superposition are shown in Figures 1–4, where all the data were reduced to 30°C .

The extent of the time-shift was rather small; for the data of 30 – 120°C , the frequency range was extended only about one decade to lower frequencies. This is because the glass-transition temperature of *cis*-polybutadiene is very low, -110°C . All master curves approach the plateau region at the higher frequencies. The lower frequency region is the transition from the plateau towards terminal region. However, these curves do not show a cross-over of G' and G'' . They are almost parallel to each other. This indicates that all these samples have some branching. However, the branching is not extensive enough to form gels as will be stated later. In Figure 5, G' curves of the four samples are compared. The curve of CB11 shows smaller slope and higher G' than those of the other samples at low frequencies. This indicates that CB11 contains a structure having longer relaxation times compared, for example, to CB24. This cannot be explained from the differences in molecular weight and its distribution because CB24 has higher molecular weight and broader molecular weight distribution than CB11 (Table I). Therefore, this must be the effect of more extensive branching in CB11 than in the others. The differ-

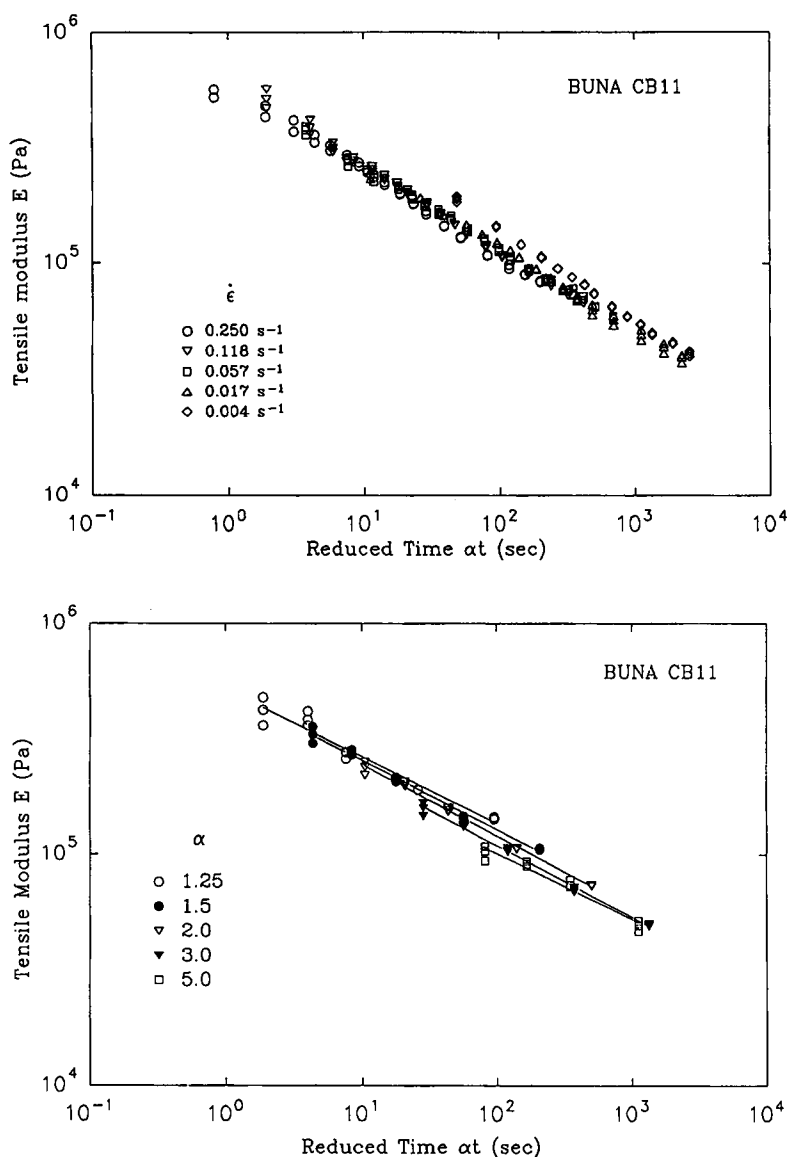


Figure 11 (a) Tensile modulus as a function of reduced time at fixed rates for CB11.
 (b) Tensile modulus as a function of reduced time at fixed extension ratios for CB11.

ences among CB22, CB23, and CB24 are related to their molecular weight distribution, and G' is higher for the higher M_n . This indicates the effect of the low molecular weight fraction on G' .

Figure 6 shows $\log G''$ versus $\log G'$ plot for the four samples. The curve of CB11 lies at the right side of those of the others. This also indicates that CB11 contains more branching than the others.¹⁷

The values of the shift factors, α_T and β_T are given in Table II. The α_T s are sample-dependent and CB11, which has the highest degree of branching, shows the highest temperature dependence. At the lower temperature CB24 shows a lower temperature

dependence than CB22 and CB23. However, the differences diminish at the higher temperature. The fact that the differences of α_T diminishes at the higher temperature indicates that the constraints introduced by the branching become less effective at the higher temperature. The observed values of β_T (Table II) are comparable to the values of $\rho_0 T_0 / \rho T$. No further significant information was obtained from β_T . From the result mentioned above (Fig. 6 and Table I), the order of degree of branching is $\text{CB11} > \text{CB22} = \text{CB23} > \text{CB24}$.

Figure 7 shows the absolute values of complex viscosity, $|\eta^*|$, of the samples at 30°C . As observed

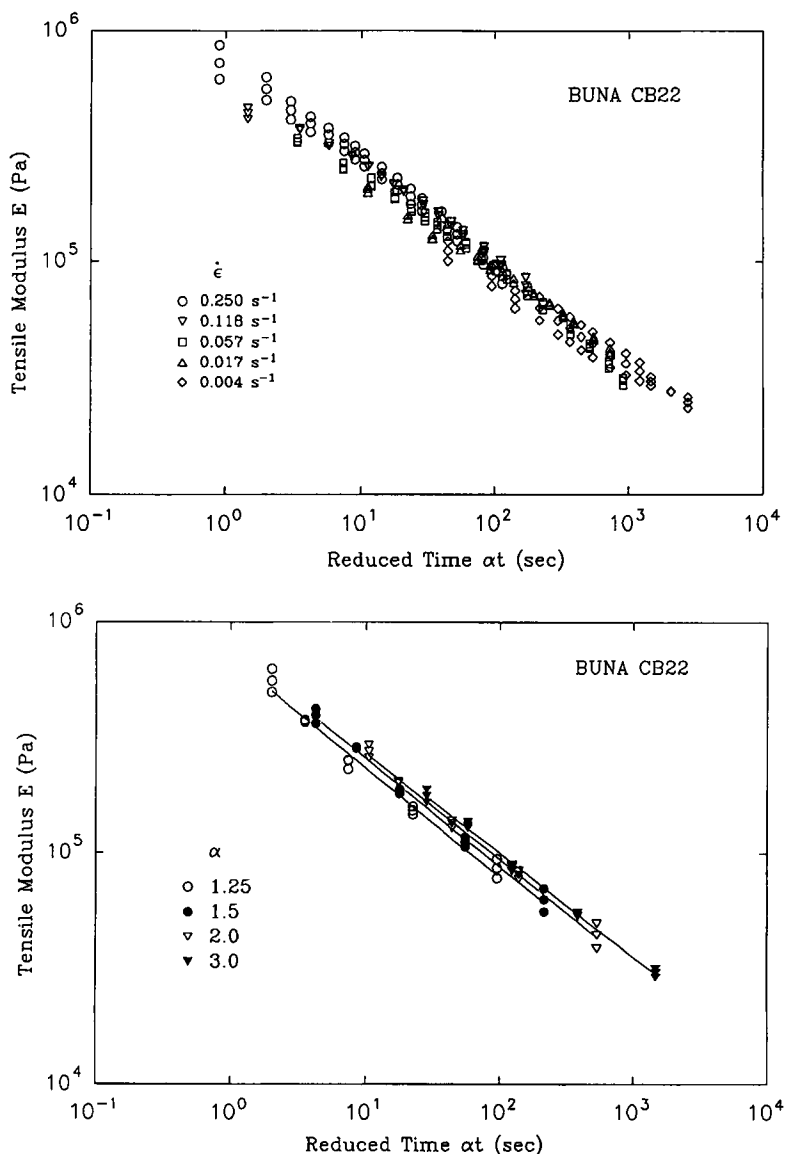


Figure 12 (a) Tensile modulus as a function of reduced time at fixed rates for CB22. (b) Tensile modulus as a function of reduced time at fixed extension ratios for CB22.

in many commercial rubbers, these do not show the Newtonian region within the observed time scale because of their high molecular weight, broad molecular weight distribution, and branching. At low frequencies, they show the viscosity enhancement resulting from branching, which is longer than the critical length.¹⁷ The sample of CB11, in spite of having the same M_w as those of CB22 and CB23, shows the highest degree of the viscosity enhancement at low frequencies and the viscosity reduction at high-frequencies; that is, the curve of CB11 crosses over the other curves. This also indicates that CB11 has more extensive branching compared

to other samples.¹⁷ For CB22, CB23, and CB24 the magnitude of $|\eta^*|$ is in the order of number average molecular weight, M_n (Table I).

TENSILE STRESS-STRAIN MEASUREMENTS

Figures 8 and 9 show tensile stress-strain curves of CB11 and CB24 at various deformation rates. The *filled circles* show the data at break. Reproducibility shown in the figures is less than $\pm 15\%$. The modulus increases with increasing deformation rates.

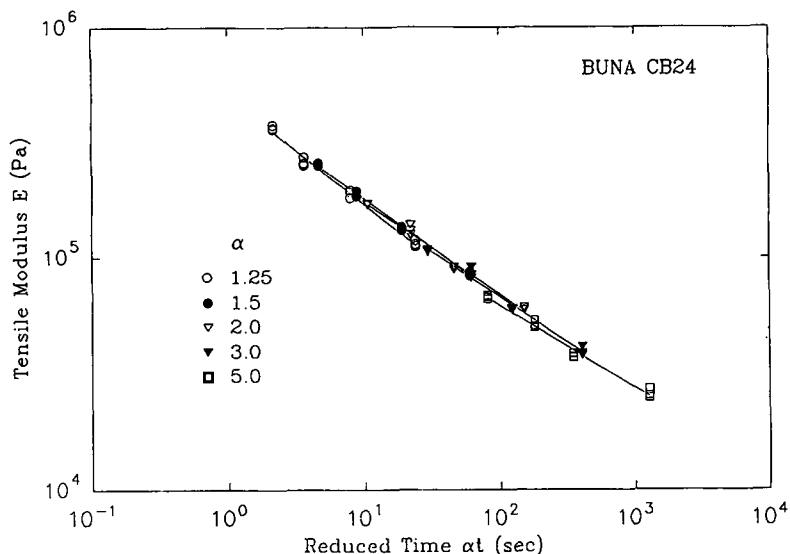


Figure 13 Tensile modulus as a function of reduced time at fixed extension ratios for CB24.

Figure 10 shows the plots of tensile modulus, $E(t)$, against time, t , at various deformation rates for CB24. The data obtained at different deformation rates do not give a master curve, because the behavior is not linearly viscoelastic.¹⁸

Figures 11–13 show the plots of tensile modulus, $E(\alpha t)$, against reduced time, αt ; as was given by eq. (4). In Figures 11(a) and 12(a) the data are plotted for each strain rate, and in Figures 11(b), 12(b), and 13 the lines are for constant values of α . CB11 and CB22 show systematic relation with

α while CB24 gives a master curve which is independent of α . With CB11 the deviation is in the direction of strain-softening and for CB22 and CB23 it is strain-hardening. Among CB22, CB23, and CB24 the extent of the strain-hardening relates to the amount of branching given in Table I. Even though CB11 has the highest amount of branching, it shows strain-softening behavior. We note that CB11 is made with a catalyst system different from that used for the other systems (Table I). Evidently, the branches of the polymer

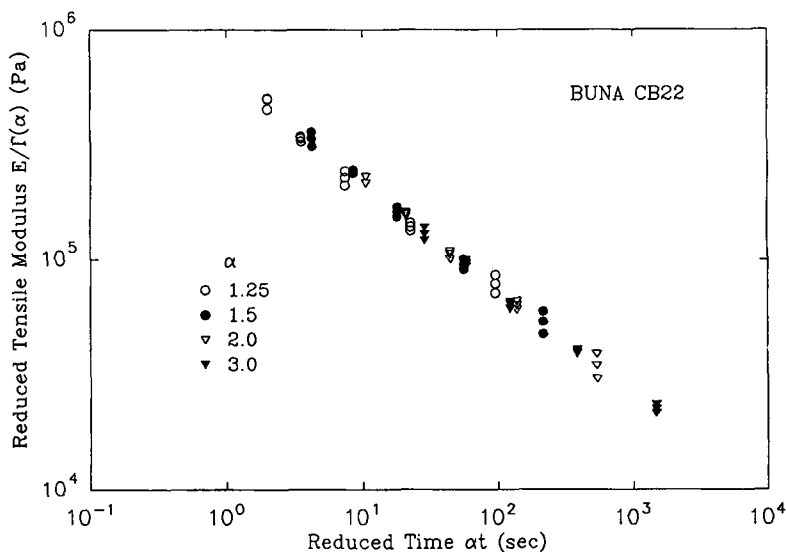


Figure 14 Reduced tensile modulus as a function of reduced time for CB22.

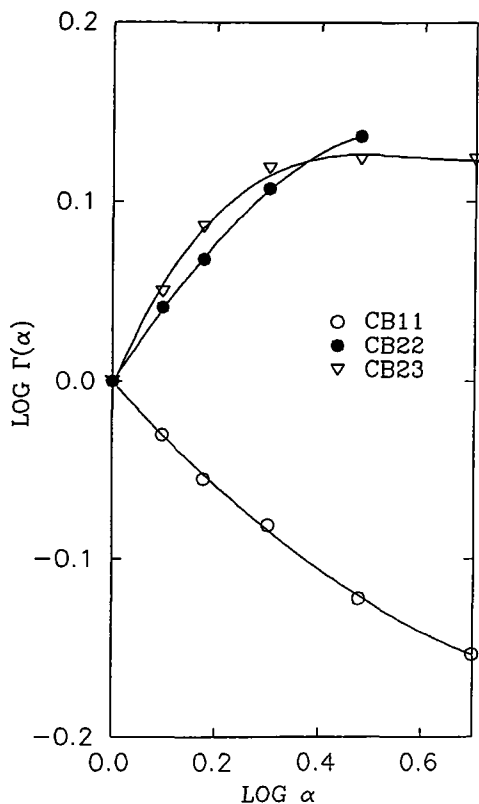


Figure 15 Modulus shift factor as a function of extension ratio.

are not long enough to provide the constrained entanglement upon stretching.

When the modulus shift,¹⁹ eq. (7), is applied, master curves are formed for CB11, CB22, and

CB23. Figure 14 shows the result for CB22. With the emulsion-polymerized rubbers, the modulus shift was required only when an extensive amount of macrogel was present.²⁰ However, there are no gels in the present samples. This is the first time when we observed strain hardening for the sample containing no gel.

Figure 15 shows the modulus shift, $\Gamma(\alpha)$, for the sample of CB11, CB22, and CB23 as a function of extension ratio. In this Figure, no data for CB24 are shown. Although CB24 has long branching, it shows neither strain-hardening nor strain-softening. This indicates that it has the critical length of branching dividing strain-hardening and strain-softening. At this critical branch-length, branches no longer contribute to such behavior as strain-hardening or softening.

Figures 16–19 show comparisons between the complex viscosity, $|\eta^*|$, and the equivalent shear viscosity, η_T , calculated from the tensile stress-strain data. The calculation of η_T for CB11, CB22, and CB23 includes the modulus shift. The values of η_T are higher than those of $|\eta^*|$ for CB11 and CB24. These results indicate that the deformational modes are different for shear and extension. η_T for CB11 and CB24 tends to converge with $|\eta^*|$ at the higher reduced rate, i.e., at smaller deformation. With CB22 and CB23, the values of η_T agree with $|\eta^*|$. The above disagreement between η_T and $|\eta^*|$ indicates strain-induced crystallization at the larger deformation. The rubber, CB11, was previously shown to give the strain-softening, and CB24 neither soft-

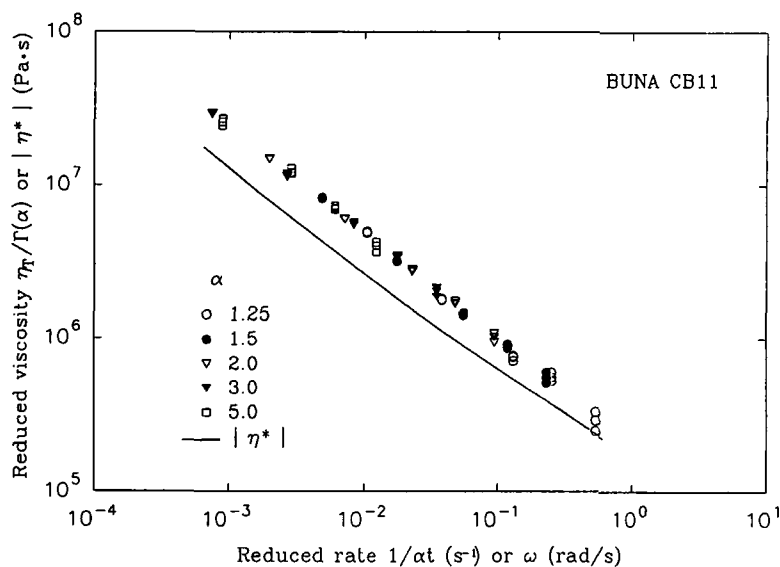


Figure 16 Comparison of complex shear viscosity with corresponding viscosity calculated from tensile data for CB11.

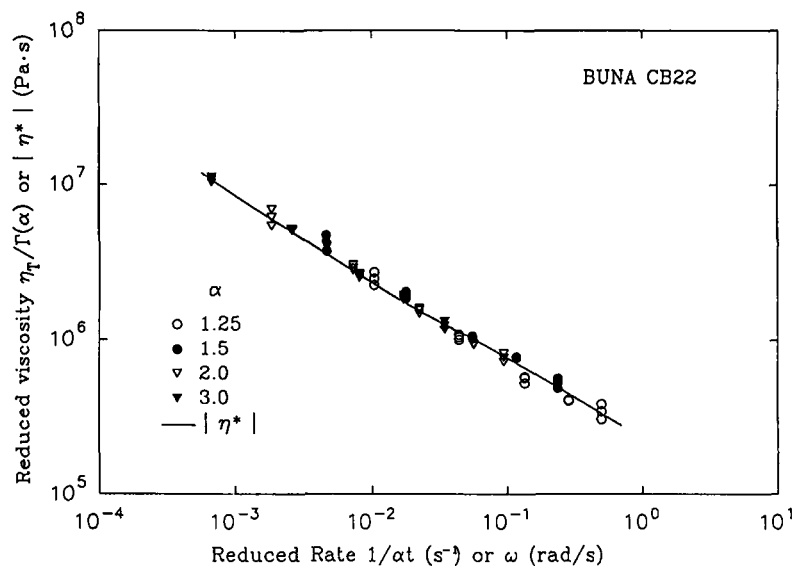


Figure 17 Comparison of complex shear viscosity with corresponding viscosity calculated from tensile data for CB22.

ening nor hardening. The implication is that easily stretchable rubbers crystallize more easily upon straining. At present we do not know why strain-induced crystallization does not appear as strain-hardening. The results of this work show that the effect of branching and that of strain-induced crystallization are observable separately, which fact is an obvious advantage in analyzing the behavior.

CONCLUSION

Deformational behavior of four commercial high-cis polybutadienes was examined with oscillatory shear measurements at small deformation and tensile stress-strain measurements at large deformation. The primary interest was to examine the effect of the long-branching structure on the above defor-

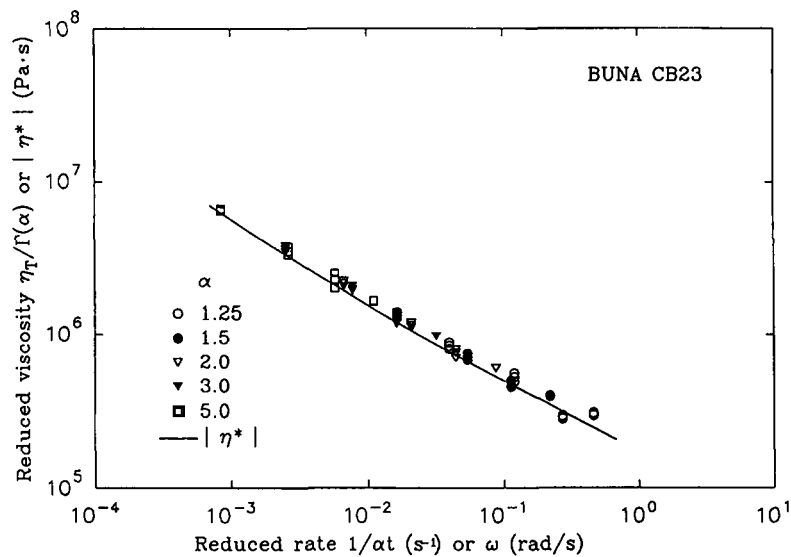


Figure 18 Comparison of complex shear viscosity with corresponding viscosity calculated from tensile data for CB23.

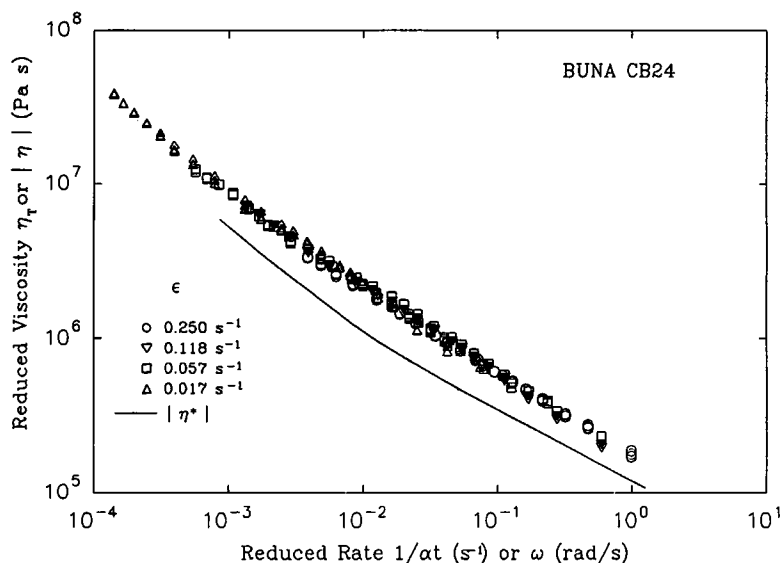


Figure 19 Comparison of complex shear viscosity with corresponding viscosity calculated from tensile data for CB24.

mational behavior, which was characterized with the dilute solution viscosity.

When the data of $\log G''$ were plotted against those of $\log G'$, rubbers were classified into two groups depending on their polymerization conditions; one group was polymerized with a Ti catalyst system and the other with Nd. The rubber polymerized with Ti had the highest degree of branching as evaluated from the dilute solution viscosity. The rubbers polymerized with Nd had the lower degree of branching; differences of the degree of branching among the Nd-polymerized rubbers were not apparent in $\log G''$ versus $\log G'$ plot.

The temperature dependence of the shift-factor in the time-temperature superposition was more sensitive to the degree of branching than the $\log G''$ versus $\log G'$ presentation. A higher temperature dependence was shown for the sample with the higher degree of branching.

The tensile measurements showed strain-hardening for two rubbers, no-strain-hardening for one rubber, and strain-softening for another. The extent of hardening or softening was assessed as the deviation from the strain-time correspondence. Among the Nd-polymerized rubbers the most highly branched sample gave the strain-hardening. In this case branches were long enough to give "constrained" entanglements. The Ti-polymerized rubber showed strain-softening, in spite of it having the highest degree of branching as evaluated from dilute solution viscosity. Here, however, the branches are

not long enough to give "constrained" entanglements and they facilitate elongation by "lubrication." Evidently, dilute solution viscosity was inadequate for characterization of the branch structure. The observed differences in the deformational behavior are related to the details of the structure, such as the density and length of branches.

The complex shear viscosity $|\eta^*|$ and the viscosity calculated from the tensile behavior, η_T , agreed with each other for two Nd-polymerized rubbers, those having the strain-hardening type of branching. The η_T was higher than $|\eta^*|$ for the strain-softening type rubber (Ti) and for one Nd-rubber, giving neither strain-hardening nor strain-softening. The difference between η_T and $|\eta^*|$ was attributable to strain-induced crystallization. The easily stretchable rubbers crystallize more easily upon stretching.

The authors express their appreciation to Yokohama Rubber Company for their financial support.

REFERENCES

1. J. T. Gruver and G. Kraus, *J. Polym. Sci.*, **2**, 797 (1964).
2. G. Kraus and J. T. Gruver, *J. Polym. Sci.*, **3A**, 105 (1965).
3. G. Kraus and K. W. Rollmann, *J. Polym. Sci.: Symposium*, **48**, 87 (1974).

4. J. M. Carella, J. T. Gotro, and W. W. Graessley, *Macromolecules*, **19**, 659 (1986).
5. N. Nakajima, E. A. Collins, and H. H. Bowerman, *Rubber Chem. Technol.*, **47**, 318 (1974).
6. N. Nakajima and E. R. Harrell, *Rubber Chem. Technol.*, **56**, 1019 (1983).
7. N. Nakajima and E. R. Harrell, *Rubber Chem. Technol.*, **59**, 305 (1986).
8. N. Nakajima and J. J. Scobbo, Jr., *Rubber Chem. Technol.*, **60**, 742 (1987).
9. P. J. Flory, *Principles of Polymer Chemistry*, Cornell University Press, Ithaca, New York, 1953, Chap. 9.
10. W. O. Baker, *Rubber Chem. Technol.*, **22**, 935 (1949).
11. L. J. Kuzma and W. J. Kelly, *Encyclopedia of Chemical Technology*, 3rd ed., Vol. 8, p. 555, Wiley, New York, 1978.
12. H. L. Hsieh and H. C. Yen, *Rubber Chem. Technol.*, **58**, 117 (1985).
13. H. Fries and B. Stollfuss, *Paper Presented at the Meeting of the Rubber Division, ACS, Cincinnati, Ohio*, Oct. 18-21, 1988.
14. W. W. Graessley, *Adv. Polym. Sci.*, **16**, 1 (1974).
15. W. W. Graessley, *Acc. Chem. Res.*, **10**, 332 (1977).
16. P. G. deGennes, *J. Phys. (Paris)*, **36**, 1199 (1975).
17. N. Nakajima and E. R. Harrell, *J. Appl. Polym. Sci.*, **29**, 995 (1984).
18. T. L. Smith, *Trans. Soc. Rheol.*, **6**, 61 (1962).
19. N. Nakajima, *Rubber Chem. Technol.*, **53**, 14 (1980).
20. N. Nakajima, C. D. Huang, J. J. Scobbo, Jr., and W. J. Shieh, *Rubber Chem. Technol.*, **62**, 343 (1989).

Received January 31, 1996

Accepted March 25, 1996